ACS APPLIED MATERIALS & INTERFACES

RESEARCH ARTICLE

www.acsami.org

Electropolymerized Molecularly Imprinted Polymer Films of a Bis-Terthiophene Dendron: Folic Acid Quartz Crystal Microbalance Sensing

Dahlia C. Apodaca,[†,‡] Roderick B. Pernites,[†] Ramakrishna R. Ponnapati,[†] Florian R. Del Mundo,[‡] and Rigoberto C. Advincula*[,†,‡]

[†]Department of Chemistry and Department of Chemical and Biomolecular Engineering, University of Houston, Houston, Texas 77204-5003, United States

[‡]Institute of Chemistry, University of the Philippines, Diliman, Quezon City, Philippines 1101

Supporting Information

ABSTRACT: A folic acid sensor was prepared via an electropolymerized molecularly imprinted polymer (E-MIP) film of a bis-terthiophene dendron on a quartz crystal microbalance (QCM). The cyclic voltammetry (CV) electrodeposition of the imprinted polymer film was monitored by electrochemical QCM or E-QCM, enabling in situ monitoring and characterization of E-MIP film formation and the viscoelastic behavior of the film. A key component of the E-MIP process is the use of a bifunctional monomer design to precomplex with the template and function as a cross-linker. The complex was electropolymerized and cross-linked by CV to form a polythiophene matrix. Stable cavities were formed that specifically fit the size and shape of the folic acid template. The same substrate surface was used for folic acid sensing. The predicted geometry of the 1:2 folic acid/terthiophene complex was obtained through semiempirical AM1 quantum calculations. The analytical performance, expressed through the figures of merit, of the sensor in aqueous solutions of the analyte was investigated. A relatively good linearity, R^2 = 0.985, was obtained within the concentration range 0−100 μM folic acid. The detection limit was found to be equal to 15.4 μM (6.8 μg). The relative cross selectivity of the folic acid imprinted polymer against the three molecules follows this trend: pteroic acid (= 50%) > caffeine (= 41%) > theophylline (= 6%). The potential and limitations of the E-MIP method were also discussed.

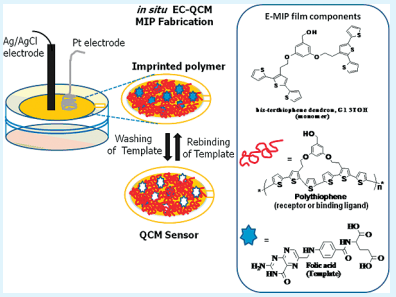

KEYWORDS: sensing, MIP, imprinting, electropolymerization, QCM, film, folic acid

INTRODUCTION

Molecular imprinting (MIP) is a technique widely used for the preparation of polymeric materials for molecular recognition.[1−4] In MIP, the specific interaction of a functional monomer with the template is manifested through the organization of specific binding sites, which usually occur during fabrication of a three-dimensional polymer monolith or film. Regardless of the type of interaction, i.e., whether covalent or noncovalent, the preorganized interaction creates a geometry that is complementary to the size and shape of the template or target molecule. This enables recognition of the template by the polymer matrix in subsequent rebinding studies or applications. MIP is a valuable component in the preparation of sensors.[5−10] The biomimetic properties of MIPs render them attractive as chemical recognition elements in sensors or artificial receptors. For recognition, MIP offers a very promising alternative to natural receptors such as antibodies and enzymes, which have relatively poor stability and a short shelf-life.[11] Because of low cost, ease of preparation, robustness, coupled with a wide choice of templates and functional monomers, and an increase in demand in the fields of food analysis, environmental monitoring, pharmaceutical assays, and security monitoring that includes the detection of explosives, chemical warfare agents, and illicit drugs,[12] MIP has become one of the most widely used methods for the preparation of sensor films.[13] However, MIP has some limitations, which include poor recognition properties in water, long equilibrium binding kinetics, and slow leaching of the template from the polymer matrix, which must be addressed appropriately.[13,14]

A main challenge in the design of MIP-based chemical sensors is that these materials are usually prepared in bulk as monoliths, thus lacking the ability to form a smooth film that is directly interfaced with a transducer or electrode. Other groups have resorted to obtaining bulk polymer films or membranes.[15−19] Another option is surface imprinting by spray- or spin-coating techniques that have been used to obtain thin films on piezoelectric devices [20]. Spin coating, in particular, often suffers from the following drawbacks: difficulty in depositing high-quality films of submicrometer thickness, tendency to form coating defects (e.g., the orange-peel effect), poor homogeneity in composition, and unwanted precipitation of the polymer due to the premature evaporation of solvents.[21] To this end, direct electrochemical deposition of polymers offers a viable means of introducing the recognition domain as films on the surface of a transducer.[22]

Received: August 29, 2010
Accepted: November 1, 2010
Published: November 16, 2010

Electrodeposition of polymers is a method for directly adsorbing an electropolymerized material on an electrode interface.[23] Electrodeposition of polymers is accomplished by either anodic or cathodic electropolymerization. These methods can be distinguished in terms of a radical-cation[24−26] (anodic) and a radical-anion (cathodic) mechanism. Also, electrodeposition, in contrast with the usual bulk polymerization, eliminates the need for rigorous synthesis and film preparation typically required by spin- or solvent-casting techniques. The film thickness and composition can be easily achieved by controlling the electrochemical parameters in cyclic voltammetry (CV) or potentiostatic deposition methods. The film thickness directly affects the sensor's response time and, hence, is a critical controlling factor for most sensing applications.[27]

Polythiophene has been one of the most notable among π-conjugated polymers[28] because of its intrinsic electrical conductivity, stability, and processability in both doped and neutral states [29]. Like polypyrrole and polyaniline, polythiophenes can be both oxidatively or reductively doped in a proper solvent.[30] The presence of sulfur in polythiophenes also enables it to be reduced and thus n-doped.[28] Significantly, polythiophenes can be straightforwardly synthesized using anodic electrodeposition techniques. There have been a number of studies conducted on electrochemically prepared polythiophene films for sensing applications[31−35] Other than sensors, the high interest in polythiophene material is its potential for various applications such as smart coatings, organic light-emitting diodes, photovoltaics, and electrochromic windows.[36−38]

Though a range of MIP-based chemosensors have already been devised,[39−41] the electrochemical approach in tandem with the MIP process has not been largely explored because of issues pertaining to homogeneous film formation and difficulty in in situ characterization.[42] Also, the possible interference or degradation of the template/analyte with the electropolymerization process is a main concern. It is important, therefore, to develop an MIP method in which the template can be protected and an in situ monitoring method be employed to characterize the MIP process. Although it is possible to monitor the MIP process primarily by electrochemical analysis (current versus potential or $I-V$) measurements, hyphenated techniques with a quartz crystal microbalance (QCM)[43,44] and surface plasmon resonance (SPR) spectroscopy[45−48] are attractive. Electrochemistry coupled with QCM, which is also known as E-QCM, as well as electrochemistry in tandem with SPR, or simply termed E-SPR, should enable the in situ growth monitoring of the MIP films on a gold electrode surface [49−52]. For E-QCM, the frequency (mass) and viscoelastic behavior of the film can be monitored simultaneously during electrodeposition.[53,54] At the same time, $I-V$ or $I-T$ (current versus time) measurements can be made because the Au-QCM electrode is also a working electrode for a three-electrode cell electrochemical setup.

Folic acid (also known as folacin and folate) is an important nutrient for the human body because it plays an essential role in the synthesis of purines and pyrimidines for DNA and in cell replication. By chemical structure, it belongs to a group of heterocyclic compounds based on the 4-[(pteridin-6-ylmethyl)-amino]benzoic acid structure. It plays a vital role in tissue growth and the formation of red blood cells. A number of studies have focused on its ability to act as an optimal targeting ligand for imaging and cancer therapy.[55] Folic acid is known to exhibit a high affinity to folate receptors ($K_d \approx 1 \times 10^{-10}$ mol/L), which makes it very attractive for targeting cytotoxic agents.[56,57]

As a nutraceutical additive, folic acid is also routinely measured in food and biological samples. There is a need to monitor its concentration in fortified foods in compliance with government regulations and product monitoring.[58,59] The standard microbiological assays commonly used for routine analysis of folic acid are based on light-scattering dispersion of the flocculent growth of the organisms *Lactobacillus helveticus* and *Streptococcus faecalis* in a folate-enriched media.[60−63] However, these are not sensitive to various chemical forms of the vitamin.[64] Others have used a wide range of analytical techniques, including polarographic methods, which is the official method used in Russian pharmacopoeia.[65] Fluorimetric procedures have found useful application in determining folic acid in natural extracts and yeasts.[66] A colorimetric method based on color development with 1,2-naphthoquinone-4-sulfonic acid, sodium salt, has been used successfully for assaying folic acid tablets containing folic acid alone or in combination with iron and vitamin B_{12}.[67]

In this study, electropolymerized molecularly imprinted polymer (E-MIP) films based on polyterthiophenes were used to generate a folic acid QCM sensor (Figure 1). In principle, the E-MIP film serves as a chemical recognition element directly interfaced with QCM transduction for subsequent quantification based on the frequency shift and resistance response. On the other hand, the gold surface of the QCM is also a working electrode in a three-electrode electrochemical cell setup. It is important to have the monomer complexed with the analyte, together with a cross-linker. In this case, a bis-terthiophene or bifunctional monomer derivative, 3,5-bis[[2-(2,5-dithiophen-2-ylthiophen-3-yl)ethoxy]phenyl]methanol, a dendron and simply referred to as G1 3TOH, was synthesized. A key feature of this design is that the AB_2 dendron acts as both a monomer complexing agent and a cross-linker for the MIP process. This interaction was modeled by a semiempirical AM1 quantum calculation method. Another important consideration is to monitor the deposition of the folic acid bis-terthiophene complex because it forms a polythiophene MIP matrix film.[30] This condition was largely accomplished by employing the hyphenated E-QCM setup. After electrodeposition, the analytical performance of the sensor, quantified through the figures of merit, was determined in a water/acetonitrile (ACN) (9:1, v/v) solution of folic acid. The E-MIP film was also found to exhibit comparatively high selectivity toward folic acid against structurally similar analogues. Moreover, the E-MIP film preparation has been shown to be simple and reproducible and their performance more robust than standard microbiological-based assays.

EXPERIMENTAL SECTION

Chemicals. Folic acid, tetrabutylammonium hexafluorophosphate (TBAH), and pteroic acid were purchased from Sigma-Aldrich (St. Louis, MO). All chemicals were used as received. Aqueous solutions were prepared from water purified using a Millipore (Billerica, MA) system (resistivity 18.2 MΩ·cm). The G1 3TOH AB_2 dendron was synthesized according to a literature procedure previously reported.[53,54] Briefly, ethyl 3-thiophene-3-acetate was used as the starting material to produce a G0 3TOH monomer. This was then subjected to a modified Mitsunobu etherification reaction accompanied with sonication to give the G1 3T ester monomer. The G1 3T ester was then reduced using lithium aluminum hydride to produce the G1 3TOH monomer as a pale-yellow solid in 90% yield.[68,69] In principle, the dendron synthesis can be carried out to succeeding generations, G2, G3, G4, ..., as needed in an AB_2 convergent manner.

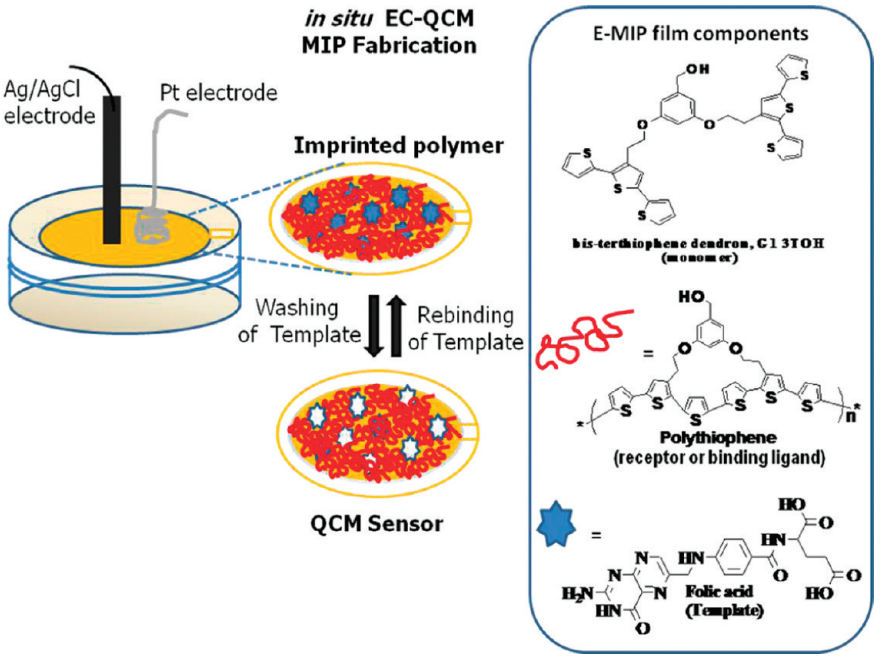

Figure 1. Schematic illustration of the fabrication of a polythiophene-based sensor for folic acid.

Instrumentation. CV was performed on an Amel 2049 Potentiostat and Power Lab system (Milano, Italy) with a three-electrode cell. The conditions and parameters for the procedure are specified in the Results and Discussion section because they vary with the experiments. EChem Windows was used to run data acquisition. This electrochemical setup is attached to a Research Quartz Crystal Microbalance (RQCM) obtained from Maxtek, Inc. (now INFICON Corp., New York). The gold surface of the QCM was used as the working electrode in the three-electrode electrochemical cell setup. The instrument is equipped with a built-in phase lock oscillator and is controlled using RQCM Data-Log Software. Prior to electropolymerization, a standard AT-cut, 5 MHz, 1-in.-diameter polished quartz crystal was cleaned in piranha solution for 60 s [1:3 (v/v) H_2O_2/H_2SO_4] and was then subjected to plasma cleaning using a March Plasmod GCM 200 (Concord, CA) for 150 s at 10 W with an argon gas purge. ***Caution!*** *Piranha solution is highly corrosive and reacts violently with organic compounds; extreme precaution must be observed in handling this solution.* QCM sensing was done by monitoring actual kinetic curves. A typical measurement for comparison was done with 100 μM folic acid in 9:1 (v/v) water/ACN, unless various concentrations were specified for sensitivity studies. The QCM curve was recorded three times with an average deviation of 5% from the shape of the curves, i.e., until a plateau is obtained, before choosing the final representative plot. The surface morphology was studied using atomic force microscopy (AFM) imaging, performed in ambient air with a PicoScan SPM system (Molecular Imaging, now Agilent Technologies, Santa Clara, CA) equipped with a 10 × 10 μm^2 scanner. Magnetic-alternating-current (MAC) mode and/or tapping mode were used for all of the AFM images. Commercially available tapping-mode tips (TAP300, Silicon AFM Probes, Ted Pella, Inc., Redding, CA) were used on cantilevers with a resonance frequency ranging from 290 to 410 kHz. For X-ray photoelectron spectroscopy (XPS), photoelectrons were collected on a Physical Electronics model 5700 XPS instrument (Chanhassen, MN) using a monochromatic Al Kα X-ray source (1486.6 eV) operated at 350 W. The analyzed area, collection solid cone, and take-off angle were set at 800 mm, 5°, and 45°, respectively. A pass energy of 11.75 eV was employed, resulting in an energy resolution of better than 0.51 eV. All spectra were acquired in vacuum (5×10^{-9} Torr or better) and at room temperature. A Shirley background subtraction routine was applied throughout the experiment. The binding-energy scale was calibrated prior to analysis using the Au $4f_{7/2}$ line. Charge neutralization was ensured through cobombardment of the irradiated area with an electron beam. Data processing was carried out using the *Multipak* software package. Ellipsometry measurements were conducted using the Optrel Multiskop (Bavaria, Germany) at an angle of 60° with respect to the surface normal and at a fixed wavelength of 632.8 nm. Δ and Ψ values were obtained for the polymer films and the clean gold-coated quartz crystal surface. The ellipsometry data were then fitted using a fitting program (Elli, Optrel), assuming a refractive index of 1.5 for the polymer layer.[70,71]

Modeling studies were performed to determine the extent of interaction that exists between the G1 3TOH monomer and folic acid. The extent of such interaction is quantified through calculated free energy changes exerted by the interacting molecules. Specifically, equilibrium geometry calculations at the ground state using the semiempirical method AM1 were carried out using *Spartan 08* (Wavefunction, Inc., Irvine, CA). It is based on neglect of the diatomic differential overlap integral approximation. Specifically, it is a generalization of the modified neglect of the differential diatomic overlap (MNDO) approximation in which the central approximation asserts that the atomic orbitals residing on different atomic centers do not overlap, thus reducing overall computations. Single-point calculations were also performed using the same theoretical model on the separate folic acid and monomer components in order to determine if the observed differences in the enthalpy of formation, ΔH_f, were induced by monomer−monomer interactions. Energy minimization was performed to obtain the initial geometries of each individual molecule and of folic acid/G1 3TOH complexes. This procedure was performed before submission of each structure for final geometry optimization. Also, a global minimum search was included in each calculation setup. Table S1 in the Supporting Information summarizes the calculated energies for the different folic acid/G1 3TOH complex systems. Briefly, just to give information on the values indicated in Table S1, the first column of values is the energy (heat of formation) of the optimized geometry of the complex formed by the interaction of folic acid with varying numbers of G1 3TOH units. On the other hand, the second column contains the sum of the energies of the individual components that make up the complex: $\sum E$(heat of formation) = $\sum E$(G1 3TOH units) + E(folic acid molecule). The third

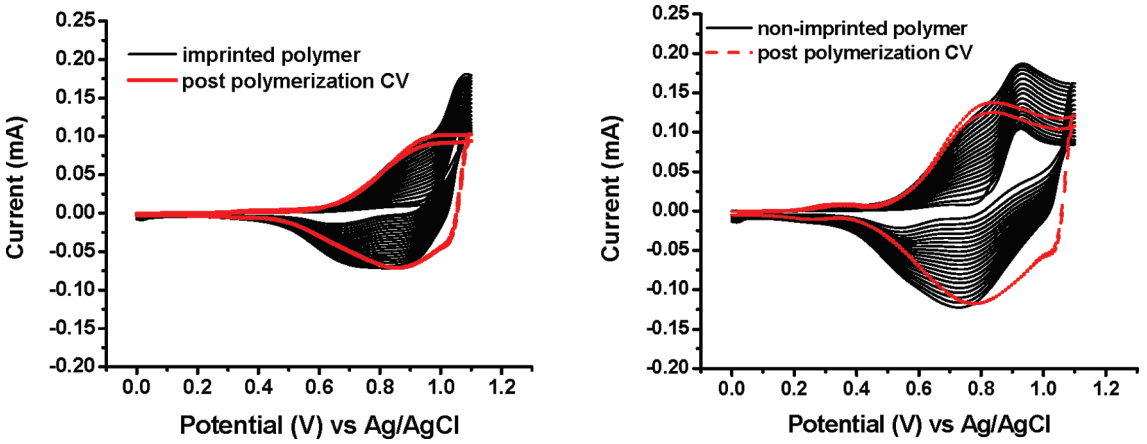

Figure 2. Cyclic voltammograms of the imprinted (a) and nonimprinted (b) polymer films: potential cycling from 0 to 1.1 V at a scan rate of 500 mV/s for 20 cycles with 0.1 M TBAH as the supporting electrolyte.

column gives the single-point energy of the G1 3TOH units calculated at different ratios, while the fourth column shows the energy of the folic acid molecule extracted from the optimized geometries for each folic acid/G1 3TOH molar ratio.

NMR spectra were recorded on a 400 MHz ^{1}H NMR General Electric QE 300 spectrometer (Fairfield, CT). UV−vis spectra were recorded using an Agilent 8453 spectrometer.

RESULTS AND DISCUSSION

Surface Imprinting by in Situ E-QCM. The formation of the nonimprinted and folic acid-imprinted polymer films was monitored in situ on the surface of a gold quartz crystal electrode by E-QCM. The E-QCM technique allows the preparation of films with varying thickness by changing the CV parameters and enables the direct deposition of the imprinted and nonimprinted polymer films onto a piezoelectric transducer surface. As shown schematically in Figure 1, a three-electrode electrochemical setup was attached to the Kynar QCM cell connected to a potentiostat. Ag/AgCl, platinum, and the gold quartz crystal were used as the reference, auxiliary, and working electrodes, respectively. Poly merization was conducted by cycling 20 times (20 cycles) the potential from 0 to 1.1 V at a scan rate of 500 mV/s (Figure 2). The MIP film was prepared from a 200 μM solution of G1 3TOH and 100 μM folic acid in ACN containing 0.1 M TBAH as the supporting electrolyte. A control polymer film, i.e., the nonimprinted polymer (NIP) film, was prepared under the same conditions but in the absence of the template (folic acid). A brown (rustlike) film was obtained from the electrochemical polymerization of G1 3TOH, with and without the template. Essentially, the brown color represents the absorption properties of a polythiophene film.[53,54]

Film formation was monitored through the changes in the current per cycle. At each CV cycle, the oxidation current increases, suggesting a stepwise growth of the polymer film. The electrochemical polymerization represents intra- and intermolecular reactions between the terthiophene units.[72] For clarity, the term polymerization indicates the formation of linear polymeric or oligomeric species mainly coming from free terthiophene or bis-terthiophene units. The term "cross-linking" refers mostly to the reaction of the terthiophene units in the template−dendron complex. The presence of folic acid as the template facilitated the creation of a polyterthiophene-based E-MIP film, which is complementary to the use of linear polythiophene for molecular recognition.[73] As a result, binding cavities, templated by the size and shape of folic acid, were formed and were used for the subsequent detection of this analyte.

It was further noted that initially two peaks seem to be observed for both voltammograms, which eventually evolved into one single peak at higher CV cycles. This could represent initially a two-electron oxidation process that later transitioned into a one-electron process. This behavior changes with the use of different solvents and/or temperature and can also be kinetically induced.[74] It is similar to what has been previously observed with polyterthiophene electrodeposition from a precursor polymer [37]. The NIP film also deposited more materials per cycle as compared to the E-MIP film, depicted by a fairly larger change in the anodic peak current. Table S2 in the Supporting Information provides a summary of the electrochemical data obtained for the deposition of MIP and NIP polymer films on the QCM gold surface.

While CV clearly illustrates the successful deposition of E-MIP films, interfacing it with QCM permits the correlation of electrochemically induced mass changes on the quartz crystal electrode per CV cycle.[75−77] Simultaneous with the reduction and oxidation peaks on the voltammograms, the changes in the frequency of the quartz crystal electrode were also obtained from the QCM, which, in turn, can be translated into the corresponding deposited mass arising from polymer film formation, through the Sauerbrey equation[78]

$$\Delta f = -2f_0^2 \Delta m / A(\rho_q \mu_q)^{1/2} \quad (1)$$

where f_0 is the fundamental resonant frequency of the QCM (5 MHz), A is the area of the electrode (1.327 cm^2), ρ_q is the density of the quartz (2.65 g/cm^3), and μ_q is the shear modulus of the quartz (2.95 × 106 N/cm^2). The negative sign in the equation signifies that, as the film is deposited on the gold surface of the QCM crystal during electropolymerization, the corresponding frequency of the crystal decreases.[53,54] Moreover, this equation can also be used in translation of the changes in frequency observed during the doping and dedoping (oxidation and reduction) processes to mass transport. To clearly illustrate the doping and dedoping processes, during the anodic cycle (oxidation), the polyterthiophene film is deposited simultaneously with doping of hexafluorophosphate counterions, which constitutes a corresponding decrease in the frequency due to an increase in mass. On the other hand, during the cathodic cycle

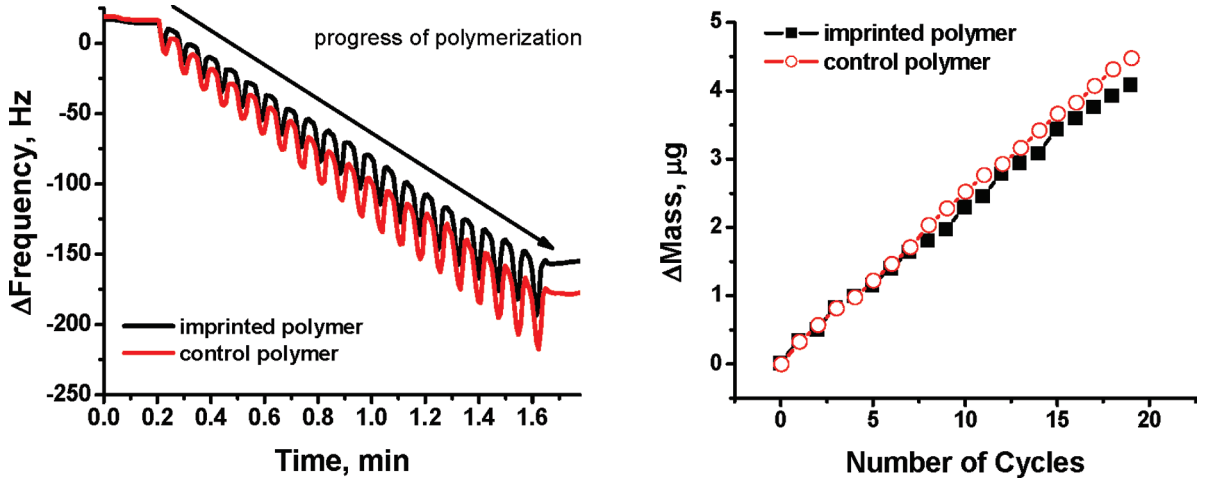

Figure 3. QCM response during electropolymerization: (a) plot of the change in frequency as a function of time; (b) plot of the change in mass against the number of CV cycles. The mass was converted using the Sauerbrey equation.

(reduction), the change in the frequency (increase) is due to dedoping of ions, indicating a decrease in mass.[53,54]

As shown in Figure 3, as electropolymerization progresses, the change in the amplitude of the oscillator becomes more pronounced. At the end of the 20th cycle for the MIP, the change in the frequency has reached −187.5 Hz, compared to −213.75 Hz for the NIP control polymer film. These correspond to a higher surface mass density for the control NIP film relative to the imprinted MIP film, i.e., 3.5 μg/cm^2 (A_q = 1.327 cm^2) against 3.1 μg/cm^2. A plot of the change in mass deposited at each cycle is given (Figure 3). What is common for both MIP and NIP films is that the mass deposition is well behaved and gives a linear growth rate coincident with a highly reversible redox behavior.

In E-MIP, the viscoelastic property may be an important issue for the polymer matrix, which provides support for the formation of binding sites and access by the analyte. Coupling the electrodeposition process with the QCM technique enables determination of the changes in the damping resistance. A change in the damping resonant resistance usually accompanies changes occurring on the surface of the quartz crystal such as adsorption, antibody−antigen interaction, and others. Thus, we attempted to correlate viscoelastic property changes concomitant with the electrochemical polymerization process. Changes on the motional resistance, ΔR, can be used to validate the formation of a structured template complex and film thermomechanical stability. E-MIP films may be gauged as stable if it is rigid enough to maintain the structure of the cavities after template removal, yet elastic or porous enough to allow high reuptake of the template. This should be possible with the right balance of linear polymerization and cross-linking reactions during the imprinting process.

We obtained a plot of ΔR as a function of ΔF for the E-MIP and control NIP films under the same conditions: 20 cycles and 0.1 M concentration in TBAH (Figure 4). The results show that, as the polymer film grows by CV, a smaller ΔR vs ΔF change is observed for the MIP film compared to the NIP film. Assuming that the template−dendron complex (prepolymer interaction[79]) has been preserved during the electropolymerization process, this indicates a more rigid film compared to the NIP film, which does not incorporate any template molecule. The reaction is primarily dominated by cross-linking of the terthiophene units both inter-and intratemplate.[80] During cycling in ACN (termed as template solvation[81]), the functional groups responsible for

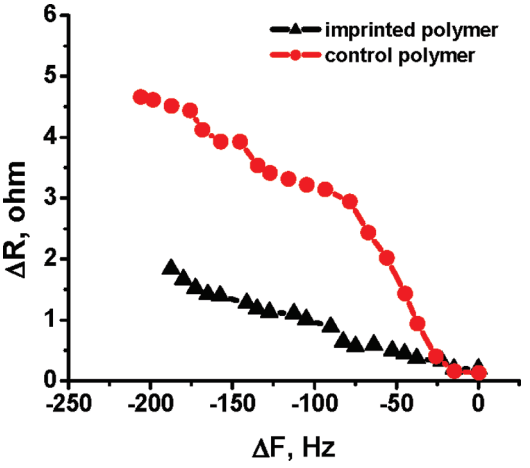

Figure 4. Illustration of the viscoelastic behavior of the nonimprinted and imprinted polymer films.

the template−dendron interactions should retain its stable arrangement, e.g., stable hydrogen-bonding arrangement, because the polar ACN is not expected to disrupt the stronger donor−acceptor hydrogen-bond pairing of the template−dendron complex. If this is the case, then the MIP film deposited on the gold surface should retain the shape and, subsequently, the cavity of the template. The fact that MIP contains a smaller amount of the terthiophene/volume but still retains a rigid viscoelastic response compared to NIP suggests that this template−dendron complex was effective in making the terthiophenes available for cross-linking,[68,69] thus yielding a high number of fidelity sites for binding [82]. On the other hand, more linear polythiophene species will then be expected from the NIP film, which would mean fewer thermosetting properties of a cross-linked system. The result is a more lossy film behavior. The CV behavior verifies the formation of more linear polythiophene species for NIP as discussed previously based on differences in the onset oxidation potential and current/cycle.

The demonstrated differences in structural rigidity between the MIP and NIP films may also be validated by the difference in mass density, with the NIP film having a higher surface mass density. The template−dendron complex in the MIP film enables efficient cross-linking ability for terthiophene but at the

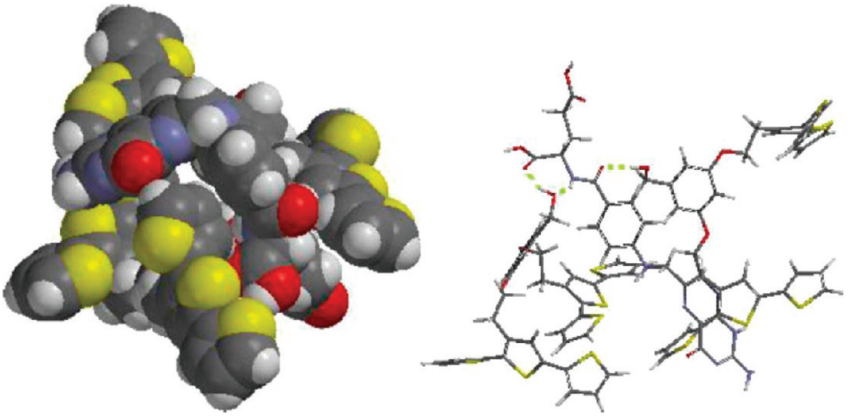

Figure 5. Predicted complex structure between folic acid and G1 3TOH (1: 2 ratio) within the imprinted polymer matrix (space filling model, left image) through AM1 semiempirical calculations using *Spartan 08* (Wavefunction, Inc.).

same time reduces the amount of material deposited because the film becomes more insulating early on. In this case, the film becomes more resistant early, i.e., increases in the heterogeneous electron-transfer kinetics, current resistance, or IR drop of the film [$V_{total} = V_{across\ film} + I(R_{film} + R_{soln})$] and a decrease of the film conductivity.[83−85] This situation is favorable with the E-MIP film because a high ratio of effective imprinted sites on the sensor surface is created.[82]

Optimization of the in Situ E-QCM Method. The in situ E-QCM method is a convenient technique for introducing and monitoring E-MIP deposition directly on the surface of an electrode/transducer. For sensing applications, optimization of the film/transducer interface requires a large surface/volume ratio capable of providing fast rebinding kinetics[86] and should be robust and even reusable. Interplay between the surface mass density and thickness may also have an effect on the film's response toward template molecule incorporation. A thick film will cause deep embedding of binding/active sites, resulting in the poor removal of the template as well as poor accessibility of the cavities for diffusion.[87]. Thus, to further explore this potential and utilize the capabilities of in situ E-QCM monitoring, we directed our efforts to optimizing the parameters commonly associated with electrochemical deposition. Particularly, we have looked into the effect of the following parameters: template−monomer ratio, scan rate, and thickness on the resulting E-MIP film using the relationship of ΔR vs ΔF.[88,89] Consequently, we correlated the viscoelastic properties to explain the observed sensitivity and selectivity toward folic acid by the E-MIP film.

In view of the results obtained from optimization experiments (relevant data shown in Figures S2−S4 and Table S3 in the Supporting Information), it may be expressed that an ideal E-MIP film should be a compromise between the right viscoelastic behavior and electropolymerization conditions (e.g., template−monomer ratio, scan rate, and solvent) to effect template removal and analyte rebinding. At the same time, this should be thin enough to have very good coupling with the transduction mechanism and analyte access. This compromise seemed to have been achieved by the following conditions: 1:2 template−monomer ratios, scan rate of 500 mV/s, use of a 200 μM solution of G1 3TOH and 100 μM folic acid in ACN containing 0.1 M TBAH as the supporting electrolyte, and finally a thickness of ~25 nm. From henceforth, all films prepared for further studies on the sensitivity and selectivity of the MIP films was done using these conditions.

Theoretical Modeling of the Template−Monomer Complex. To further confirm the importance of the 1:2 template−dendron ratio previously discussed, a theoretical model of the 1:2 folic acid/G1 3TOH complex was obtained from semiempirical AM1 calculations using *Spartan 08*, as shown in Figure 5. This predicts the possible arrangement of the dendron and template within the network (Figure S5 and Table S1 in the Supporting Information). The interaction energy between G1 3TOH and folic acid was obtained from calculated heats of formation using eq 2.

$$\Delta E = E_{\text{folic acid/G1 3TOH complex}} - [E_{\text{G1 3TOH}} + E_{\text{folic acid}}] \quad (2)$$

A negative value for ΔE denotes favorable interaction between the monomer and target analyte.[90−92] The calculated interaction energy for such a conformation or arrangement of the G1 3TOH/folic acid complex is −53.8785 kJ/mol, suggesting that a relatively stable complex is formed between G1 3TOH and folic acid. As displayed in the space-filling figure, the two monomer units of G1 3TOH are arranged in an intertwined manner, creating a cross-linkable conformation, with folic acid (template) being sandwiched by these monomer units. The proposed arrangement of the molecules may have been made possible by a hydrogen-bonding interaction providing such stability to the formed complex between G1 3TOH and folic acid. In particular, a favorable donor−acceptor hydrogen bonding between the oxygen atoms in the HO− of the G1 3TOH monomer and the hydrogen atoms of the amine groups of the template (folic acid) is possibly formed as implied by the calculated bond distances. To effect hydrogen-bond formation, calculated bond distances due to hydrogen bonding (represented by broken lines) must be less than or equal to 2.00 Å. The calculated bond distances for the hydrogen bonds formed between atoms of G1 3TOH and folic acid were found to be as follows: 1.755, 1.916, and 2.028 Å.

To further affirm template−monomer interactions in a folic acid−terthiophene dendron system, NMR and UV−vis studies[93−96] were also performed. NMR titration experiments have long been widely used in determining protonation sites,[97] structure and hydrogen bonding,[98,99] and association constants. In this particular experiment, increasing amounts of the G1 3TOH monomer were added to a fixed amount of folic acid. The corresponding ^{1}H NMR spectra were then measured in deuterated dimethyl sulfoxide. The interaction of folic acid with the terthiophene dendron was ascertained by noting

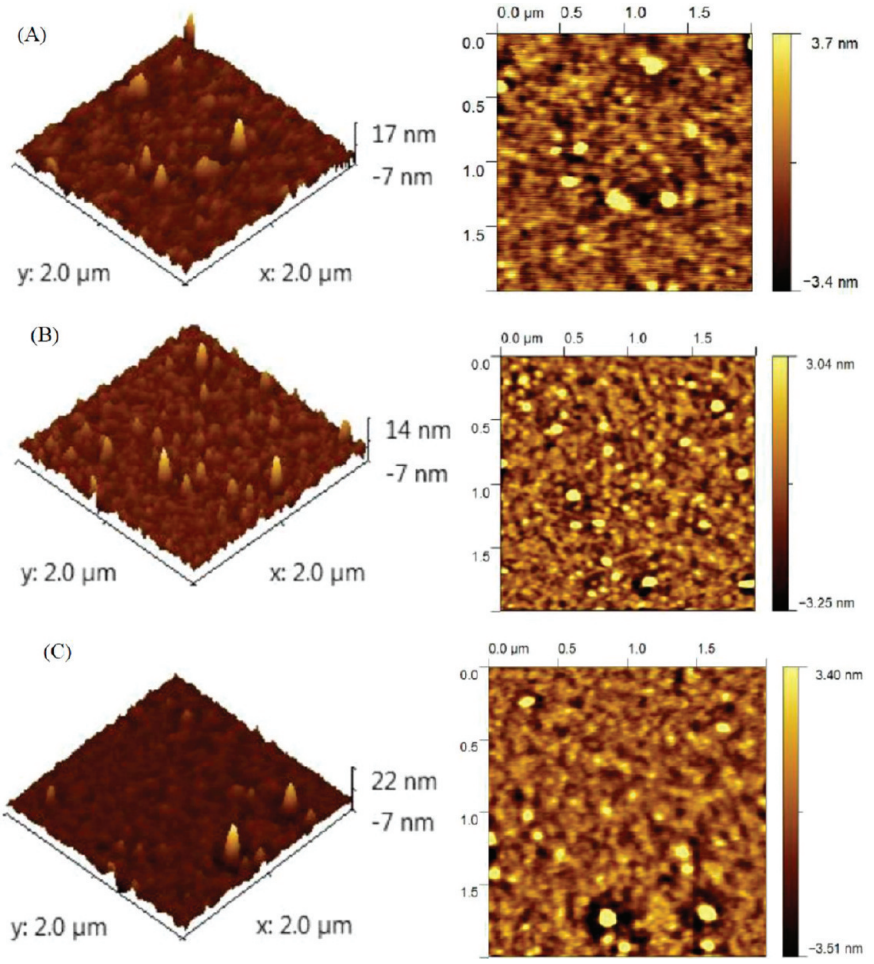

Figure 6. 3D (left) and 2D (right) AFM topography images (2 μm × 2 μm^2 scan): nonimprinted (A), imprinted (B), and imprinted polymer after template removal (C). 2D AFM amplitude and phase images are shown in Figure S9 in the Supporting Information.

the ^{1}H NMR spectral shifts of hydroxyl, amine, and the hydrogenated nitrogen atom moieties of folic acid. It was reported in a study by Sellergren et al.[93−96,100] that amine protonation is supported by an upfield shift in the ^{1}H NMR spectrum of folic acid. The shift changes are tabulated in parts a and b of Table S4a in the Supporting Information. The addition of two monomer units of G1 3TOH with folic acid yielded relatively large and significant changes in the chemical shifts of the above-mentioned functionalities.

While the NMR data further support the results of modeling studies, a UV−vis technique was also employed in this study to determine the formation constant for the most favorable template−monomer ratio and to display the binding capacity of the terthiophene dendron. The mole ratio method was employed in this particular experiment. The concentration of the G1 3TOH monomer was held constant (10^{-5} M), while that of folic acid was varied (from 1 to 10 μM). The changes in the UV−vis spectra are shown in Figure S7 in the Supporting Information, and these changes have been translated into a plot of absorbance as a function of the G1 3TOH/folic acid ratio (Figure S8 in the Supporting Information). The intersection of the two slopes from the plot implies that the 2:1 G1 3TOH/folic acid ratio yields the most pronounced spectral change. It is assumed that, in the presence of folic acid, conformational changes may have occurred, causing alterations on the disordered, aggregated structure of the terthiophene units. This, in turn, resulted in an observed increase in the absorbance and a slight shift of λ_{max}.

In summary, modeling studies coupled with NMR and UV−vis analyses provide important structural or mechanistic information on prepolymerization template−monomer complexes, which eventually lead to affinity sites in an electropolymerized terthiophene MIP film. The efficiency and selectivity of the resulting E-MIP film are dictated by the number and relative strength of this prepolymer complex or template−monomer interactions and hence must be given utmost importance for future E-MIP procedures.

AFM Morphology Studies. The AFM images, as shown in Figure 6, depict the surface topography of NIP (A), MIP (B), and MIP after template removal (C). The images were taken using a 2 × 2 μm^2 scanned area. The AFM images substantiate the E-QCM data, which suggests a successful deposition of the polymer film on the gold surface. Though the E-QCM data show that a relatively denser film is obtained in the absence of folic acid, a rather nonhomogeneous NIP polythiophene film was observed in the AFM images. This can be explained by the rapid propagation step for the polymerization and precipitation of linear polymer species from the solution.[101] This was also revealed through the observed differences in the roughness of the surfaces [expressed in terms of the root-mean-square (RMS) value]. NIP exhibited a rougher surface with a calculated RMS

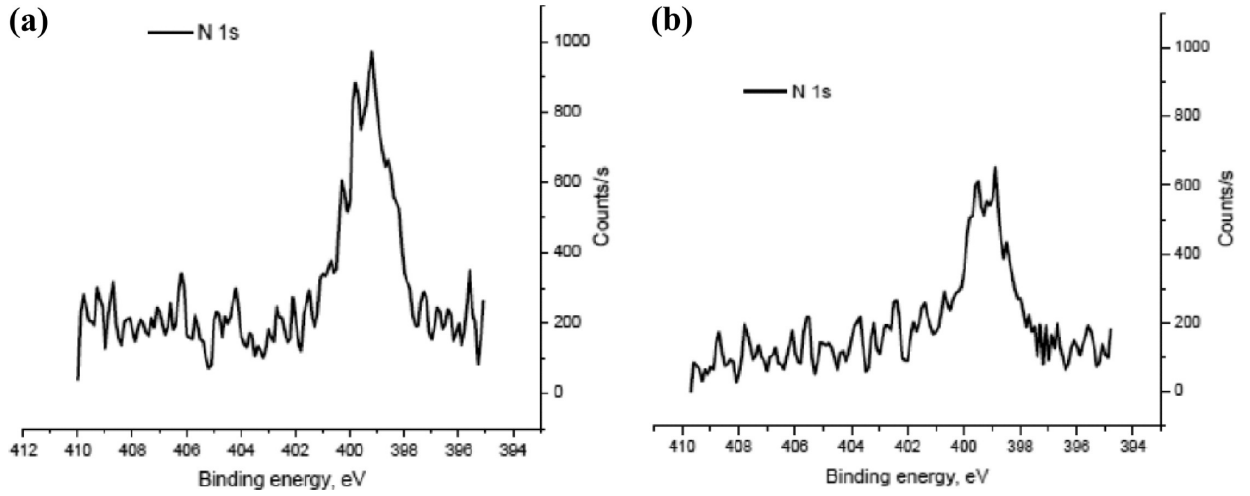

Figure 7. High-resolution XPS scan of the imprinted polymer film (N 1s) before (a) and after removal (b) of the template.

value of 1.66 nm compared to the imprinted polymer with which the template is still incorporated into the polymer network, having an RMS value of 1.38 nm. The roughness of the E-MIP film after washing with methanol/acetic acid is increased though, i.e., RMS value = 3.87 nm.

Additionally, the AFM images suggest differences in terms of the electropolymerization mechanism.[102,103] The electrodeposition of the films should be affected by the presence of the template (folic acid). The effect of folic acid on the formation of the polythiophene network may be based on the nucleation density. The AFM image of the E-MIP displays more grains on its surface compared with that of the surface of the NIP film. The occurrence of grains may be attributed to the dynamics of electropolymerization. It is well-known that both three-dimensional (3D) nucleation and two-dimensional (2D) instantaneous nucleation are involved with the electrochemical deposition process of thiophene monomers.[104] However, in the case of MIP electropolymerization, more uniform and greater numbers of nucleation sites are initially formed to give a moderately smoother surface relative to the surface of the NIP film. In the presence of these nucleation sites, the MIP film grows, as manifested by the increasing size of the domains and aggregates.[105] These grains may be attributed to aggregates formed by the template−dendron precomplex in solution and extended onto the polymer electrodeposition. Furthermore, the interaction of G1 3TOH with folic acid based on hydrogen bonding and other associated noncovalent interactions induced changes not only on monomer−monomer and monomer−solvent forces but also on the overall complex aggregate stability in solution. For some compositions and scan rates, the changes in this template−monomer complex could lead to a reduction in the amount of self-aggregation or the unsuccessful incorporation of folic acid with the polymer network. The eventual properties of the deposited film such as polymer−polymer entanglement and degree of cross-linking would also account for the ability of the polymer film to swell, thereby affecting the rebinding kinetics. With various solvent washings, these differences could be further highlighted, e.g., the AFM image of the film after methanol/acetic acid washing. Notably, the polymer film should not be excessively swollen so as to cause the collapse of the binding cavities formed during electropolymerization.

Template Removal Studies by XPS. XPS was used to confirm the successful incorporation of the template molecule on the imprinted polymer. XPS spectra were obtained from film samples electropolymerized on a gold-coated BK7 glass. Folic acid was then removed from the imprinted polymer by dissolution in a methanol/acetic acid solution (9:1, v/v), rinsed with methanol only to remove traces of acetic acid, and subsequently dried under a stream of nitrogen gas. Washing of the polymer film was done repeatedly for six consecutive times or a total washing time of at least 1.5 h. The NIP film that served as the control was also treated in the same way as the MIP film. We tracked the signal coming from the N 1s electron as a unique marker because this atom can only be associated with the template (folic acid). As shown in the N 1s spectrum of the MIP film, a band at about 398−401 eV corresponds to the nitrogen atoms of folic acid in different environments (Figure 7). Specifically, binding energies of 399.3, 398.3, and 395.7 eV correspond to the amine moiety ($-NH_2$) and nonhydrogenated (−N═) and hydrogenated (−NH) nitrogen atoms of folic acid, respectively (Figure S10 in the Supporting Information).[106,23] The deconvoluted spectrum also showed a band at 405.5 eV, which refers to the nitrogen atom of a trace quaternary ammonium cation, of the supporting electrolyte that may have been trapped in the MIP film during electrodeposition.[107]

Percentage atomic concentrations of nitrogen in the control (nonimprinted) and imprinted E-MIP films before and after template extraction are as follows: 0.10, 1.72, and 0.85, respectively. The small percentage of nitrogen obtained from the control or nonimprinted polymer may be due to the supporting electrolyte used, TBAH, during the electropolymerization process. These counterions may have been trapped within the polymer network even after the dedoping process. Removal of folic acid by methanol/acetic acid washing would only account for 50% of the folic acid present in the polymer network (Figure 7b). It should be possible to optimize template removal using a constant potential-assisted washing procedure. We also calculated the nitrogen/sulfur ratio to assess the relative effect of the washing solution on the polymer matrix. Because the percentage atomic concentration of sulfur did not change significantly (before and after template removal, the S 2p percentage atomic concentrations are 9.12 and 8.98, respectively), it can be

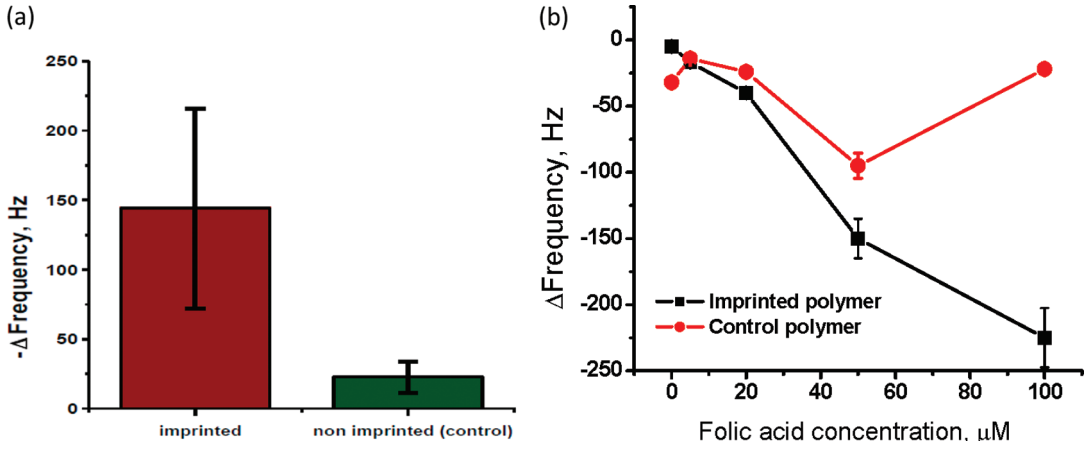

Figure 8. (a) QCM responses of both imprinted and nonimprinted sensors toward 100 μM folic acid and (b) calibration plot for the rebinding of folic acid by the folic acid-imprinted polymer.

ascertained that the polymer structure is not greatly affected by the applied methanol/acetic acid washing procedure.

Analytical Performance of the MIP/QCM Sensor . *Sensor's Response to Varying Concentrations of Folic Acid.* Figure 8a gives the QCM response of E-MIP against NIP in folic acid sensing, confirming the successful imprinting of folic acid. The imprinting factor can be calculated from the ratio of the folic acid binding capacity on the imprinted E-MIP film to that of the control NIP film.[108−112] Calculations made using the experimental results yield an imprinting factor of 3.89. The frequency shift as a function of time (kinetic curve) of the QCM is shown in Figure S11 in the Supporting Information.

The MIP film was exposed to varying concentrations of folic acid, i.e., from 0 to 100 μM, with the extent of the frequency shift being noted at each concentration. A calibration curve, illustrated on Figure 8b, was obtained from the plot of the change in frequency as a function of the folic acid concentration in micromolar. As shown in the plot, the imprinting effect is not clearly demonstrated at low folic acid concentrations; however, starting at 20 μM, the ability of the E-MIP/QCM sensor to distinguish folic acid was efficiently demonstrated. Also, from the plot, a relatively good linearity was obtained within this concentration range of folic acid with R^2 = 0.985. The detection limit,[113−116] which is defined as the minimum concentration or mass of analyte that can be detected at a known confidence level (multiple k = 3; i.e., the confidence level of detection will be 95%), was also calculated. The detection limit for folic acid sensing by the E-MIP film was found to be equal to 15.4 μM (6.8 μg) and was obtained by dividing three times the standard deviation (3σ) with the experimentally determined slope (m) of the calibration plot. Also, to verify the importance of electrodeposition of the 1:2 template−dendron ratio on the E-MIP preparation, the highest frequency shift at −275 Hz was only observed for this composition (Figure S2 in the Supporting Information). Moreover, as with the other compositions of MIP, the performance was similar to that of NIP, only up to a −25 Hz shift. Similarly, as previously discussed in the section describing the details of the optimization procedures performed, the films prepared at 500 mV/s showed the largest frequency shift at −225 Hz, as compared to the average of −50 Hz for both the MIP and NIP films prepared at lower scan rates (Figure S3b in the Supporting Information). Note that lower scan rates endow formation of a thicker polymer film. This highlighted the importance of the right thickness in achieving optimal sensitivity.

Recognition Selectivity of Folic Acid E-MIP. The selectivity of the folic acid-imprinted polymer was investigated by exposing the polymer film to a 100 μM solution each of caffeine, pteroic acid, and theophylline. The structures of these compounds (Figure 9b) are similarly related to that of folic acid. A bar chart, shown in Figure 9a, displays the observed changes in the frequency of the QCM crystal upon exposure of the E-MIP film to each solution of the competing molecule. Interestingly, the most pronounced change in the frequency of E-MIP/QCM was observed only upon binding of folic acid. The large shift with the frequency denotes that more molecules are bound onto the E-MIP/QCM sensor film, which is mainly due to the rebinding of the template molecule into the imprinted cavities within the polymer matrix. Consequently, data obtained from this plot were used to calculate the percent of cross selectivity[117,118] of the E-MIP film sensor. The efficiency of binding of folic acid to the imprinted cavities is best described by the cross-selectivity ratio. The cross-reactivity ratio is referred to as the ratio of the change in the frequency of the crystal observed upon binding of the competing molecule to the change in the frequency when the film was exposed to a solution containing the target analyte, i.e., $\Delta f_{x\ \mathrm{molecule}}/\Delta f_{\mathrm{folic\ acid}}$. The relative cross selectivity of the folic acid-imprinted polymer against the three molecules follows the trend pteroic acid (= 50%) > caffeine (= 41%) > theophylline (= 6%). A significantly small cross-selectivity ratio indicates very little and/or the absence of interaction between that of the imprinted polymer film and the competing molecule. Hence, among the three molecules subjected to rebinding, theophylline gave the poorest rebinding response with the imprinted polymer film; thus, theophylline will not significantly interfere with the sensing of folic acid. Moreover, as shown in Figure S12 in the Supporting Information, the binding of theophylline with the imprinted polymer film was unstable relative to the other molecules, as suggested by a hump in the QCM response, after about 100 min of exposure. On the other hand, pteroic acid, which also belongs to the pterin family, may potentially interfere with the sensing of folic acid.

Determining the Binding Mechanism. Changes in the QCM frequency obtained during the rebinding of different concentrations of folic acid on the imprinted polymer were used to calculate the amount of folic acid that rebinds with the imprinted polymer film. The calculated values were then used to establish the relationship of the surface mass density with the

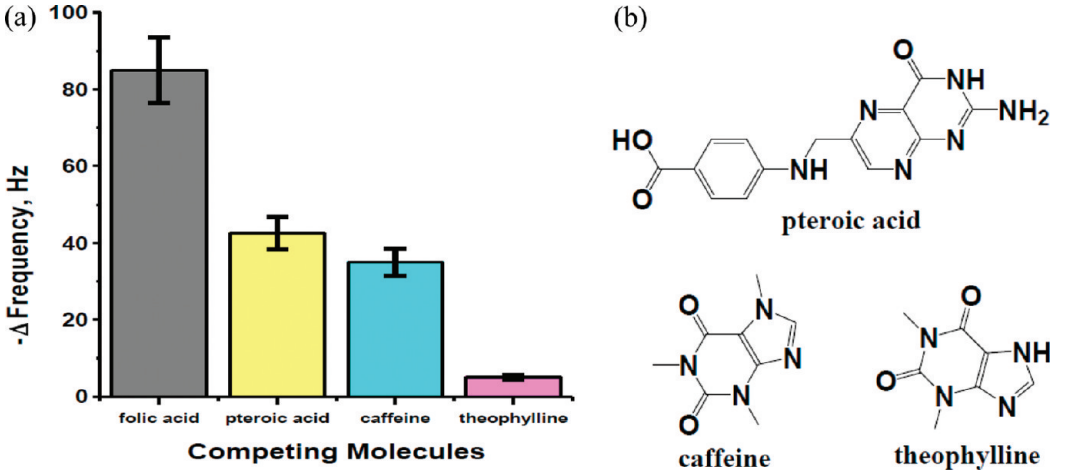

Figure 9. (a) Observed changes in the frequency of the QCM crystal (5 MHz) upon the rebinding of competing molecules: demonstrating the relative selectivity of the imprinted polymer film toward folic acid. (b) Chemical structures of the competing molecules.

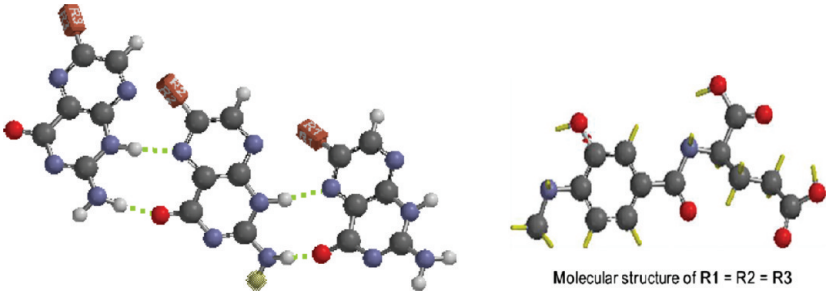

Figure 10. Illustration of the proposed cooperative binding among folic acid molecules due to hydrogen bonding (*Spartan 08*, Wavefunction, Inc.).

folic acid concentration in the bulk. This can be done by employing the Langmuir adsorption isotherm, which assumes a monolayer adsorption. The Langmuir equation adopted for this study may be expressed as

$$\frac{\Delta m}{A} + \frac{\Delta m_{\max}}{A} = \frac{C}{C + K_d} \qquad (3)$$

where $\Delta m_{\max}/A$ is the maximum surface mass density, while K_d gives the dissociation constant. However, the binding kinetics of folic acid to the imprinted polymer deviates from the Langmuir model upon fitting of the experimental data. This suggests that the binding of folic acid to the imprinted polymer involves specific adsorption or multilayer adsorption, unlike the Langmuir isotherm, which is more general for nonspecific adsorption. Instead, we used the Hill equation,[119,120] commonly applied to enzyme−substrate binding, to describe the binding event between folic acid and the imprinted polymer. Equation 4 has been modified to follow the Hill equation

$$\log(\Delta m/A) = n \log [C] - \log K_d \qquad (4)$$

where n is a constant, [C] is the concentration of folic acid in micromolar, and K_d is the dissociation constant. Fitting of the experimental data gives the equation $y = 1.018x + 1.577$ (R^2 = 0.975), indicating that cooperativity occurred during binding of the template with the polymer, commonly associated with enzyme kinetics. Moreover, the n value obtained is greater than 1, suggesting a positive cooperativity. This implies that once a folic acid molecule binds to the polymer network, its affinity for other folic acid molecules increases. It has been reported in

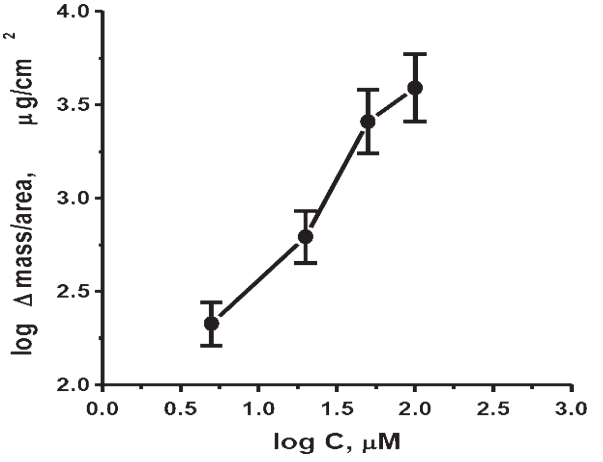

Figure 11. Plot illustrating the changes in the surface mass density of the polymer film against increasing concentrations of folic acid.

several papers that the pterin ring of folic acid possesses the potential to show two hydrogen-bonded self-assembling patterns.[121] This ability to form self-assembling patterns of hydrogen bonds is illustrated in Figure 10 (*Spartan 08*, Wavefunction, Inc.).

It can also be seen from the plot in Figure 11 that there is a small change in the surface mass density as the concentration of folic acid is varied, as manifested by the slightly sigmoidal curve. It could be that the polymer network may possess a flexible structure, induced by the presence of folic acid molecules, making the cavities reversibly accessible to the template for

binding. This means that the template has reorganized itself as it approaches the binding sites, allowing for a better fit with the preformed cavities. It must be noted, however, that the K_d value obtained from the experimental data is relatively large, i.e., 37.76 μM. At some point, folic acid molecules may tend to dissociate and to desorb from the polymer binding sites. This could possibly explain the reversible binding observed during the rebinding process.

CONCLUSIONS

On the basis of our results, we have successfully prepared a bis-terthiophene dendron-based E-MIP sensor film for the detection of folic acid with monitoring through an in situ E-QCM. It was found that the relative rigidity of the imprinted polythiophene film, prepared via optimized electropolymerization conditions, is a function of the scan rate, template−dendron composition, and thickness. Furthermore, creation of the binding sites for these artificial receptors would also depend on the affinity of folic acid toward the terthiophene dendron. This was confirmed through the existence of a favorable prepolymer complex at a 1:2 ratio. Conformational changes brought about by complexation and other noncovalent interactions were clearly demonstrated using modeling studies verified with NMR and UV−vis analyses. Moreover, these tools proved to be vital in determining the nature of the interaction, the number of binding sites, and the formation constant of the folic acid/G1 3TOH complex so as to permit the fabrication of effective E-MIP films, i.e., exhibiting sensitivity and high selectivity toward the template molecule. A relatively good linearity was achieved (R^2 = 0.985) for the rebinding of folic acid by the E-MIP/QCM film sensor within the concentration range between 0 and 100 μM. The polythiophene-based sensor also exhibited good selectivity toward folic acid as compared with structurally related compounds such as pteroic acid, theophylline, and caffeine. Indeed, the observed sensitivity and selectivity of the polythiophene-based E-MIP sensor film toward folic acid is due to optimized template−monomer incorporation in the polymer matrix and the right viscoelastic properties of the film. Moreover, a positive cooperativity occurs during the binding of folic acid as verified by semiempirical quantum calculations. Our current effort is directed toward a better understanding of the mechanism of binding, with focus on characterizing other electropolymerized imprinted polymers by other transduction methods such as the electrochemical impedance spectroscopy. Also, we are presently focused on testing this concept of electropolymerized MIP-based chemical sensors for various classes of analytes ranging from food adulterant and additives, endocrine-disrupting compounds, pesticides, illicit drugs, and explosives.

ASSOCIATED CONTENT

Supporting Information. QCM kinetic measurements, XPS deconvolution, viscoelastic plots, theoretical molecular modeling studies, etc. This material is available free of charge via the Internet at http://pubs.acs.org.

AUTHOR INFORMATION

Corresponding Author

*Phone: +1 713 743 1760. E-mail: radvincula@uh.edu.

ACKNOWLEDGMENT

The authors acknowledge funding from the National Science Foundation (ARRA CBET-0854979 and DMR-10-06776), Robert A. Welch Foundation (E-1551), and an Alliance for NanoHealth of Texas Seed grant. D.C.A. gratefully acknowledges the DOST-Philippine Council for Advanced Science and Technology Research Development for financial support. We also acknowledge technical support from INFICON Corp. and Agilent Technologies.

REFERENCES

(1) Shea, K. J.; Spivak, D. A.; Sellergren, B. *J. Am. Chem. Soc.* **1993,** *115*, 3368–3369.
(2) Yamazaki, T.; Yilmaz, E.; Mosbach, K.; Sode, K. *Anal. Chim. Acta* **2001,** *435*, 209–214.
(3) Vlatakis, G.; Andersson, L. I.; Muller, R.; Mosbach, K. *Nature* **1993,** *361*, 645–647.
(4) Cheong, S. H.; McNiven, S.; Rachkov, K.; Levi, R.; Yano, K.; Karube, I. *Macromolecules* **1997,** *30*, 1317–1322.
(5) Malitesta, C.; Losito, I.; Zambonin, P. G. *Anal. Chem.* **1999,** *71*, 1366–1370.
(6) Dickert, F. L.; Hayden, O.; Halikias, K. P. *Analyst* **2001,** *126*, 766–771.
(7) Piletsky, S. A.; Terpetschnig, E.; Andersson, H. S.; Nicholls, I. A.; Wolfbeis, O. S. *Fresenius' J. Anal. Chem.* **1999,** *364*, 512–516.
(8) Lin, J. M.; Yamada, M. *Analyst* **2001,** *126*, 810–815.
(9) Kriz, D.; Mosbach, K. *Anal. Chim. Acta* **1995,** *300*, 71–75.
(10) Sergeyeva, T. A.; Piletsky, S. A.; Brovko, A. A.; Slinchenko, E. A.; Sergeeva, L. M.; El'skaya, A. V. *Anal. Chim. Acta* **1999,** *392*, 105–111.
(11) Lou, X.; He, P.; Okelo, G. O.; He, L. *Anal. Bioanal. Chem.* **2006,** *386*, 525–531.
(12) Haupt, K.; Mosbach, K. *Chem. Rev.* **2000,** *100*, 2495–2504.
(13) Wu, X., Shimizu, K. D. In *Molecular Recognition and Polymers: Control of Polymer Structure and Self-assembly*; Rotello, V., Thayumanavan, S., Eds.; John Wiley and Sons: New York, 2008; p 397.
(14) Allender, C. J. *Adv. Drug Delivery Rev.* **2005,** *57*, 1731–1732.
(15) Nopper, D.; Lammershop, O.; Wulff, G.; Gauglitz, G. *Anal. Bioanal. Chem.* **2003,** *377*, 608–613.
(16) D'Agostino, G.; Alberti, G.; Biesuz, R.; Pesavento, M. *Biosens. Bioelectron.* **2006,** *22*, 145–152.
(17) Piletsky, S. A.; Piletskaya, E. V.; Sergeyeva, T. A.; Panasyuk, T. L.; El'skaya, A. V.; Levi, R.; Karube, I.; Wulff, G. *Macromolecules* **1998,** *31*, 2137–2140.
(18) Pogorelova, S. P.; Bourenko, T.; Kharitonov, A. B.; Willner, I. *Analyst* **2002,** *127*, 1484–1491.
(19) Sergeyeva, T. A.; Piletsky, S. A.; Brovko, A. A.; Slinchenko, E. A.; Sergeeva, L. M.; Panasyuk, T. L.; El'skaya, A. V. *Analyst* **1999,** *124*, 331–334.
(20) Dickert, F. L.; Hayden, O. *Anal. Chem.* **2002,** *74*, 1302–1306.
(21) Bai, J.; Snively, C. M.; Delgass, W. N.; Lauterbach, J. *Macromolecules* **2001,** *34*, 1214–1220.
(22) Walton, D. J.; Hall, C. E.; Chyla, A. *Analyst* **1992,** *117*, 1305–1311.
(23) Pietrzyk, A.; Suriyanarayanan, S.; Kutzer, W.; Chitta, R.; D'Souza, F. *Anal. Chem.* **2009,** *81*, 2633–2643.
(24) Skotheim, T. A. *The Handbook of Conducting Polymers*; Marcel Dekker: New York, 1986; Vols. 1 and 2.
(25) Asavapiriyanout, S.; Chandler, G. K.; Gunawardena, G. A.; Pletcher, D. *J. Electroanal. Chem.* **1984,** *177*, 229–244.
(26) Morse, N. J.; Rosseinsky, D. R.; Mortimer, R. J.; Walton, D. J. *J. Electroanal. Chem.* **1988,** *255*, 119–141.
(27) Ayad, M. M.; El-Hefnawey, G.; Torad, N. L. *J. Hazard. Mater.* **2009,** *168*, 85–88.
(28) Teasdale, P. R.; Wallace, G. G. *Analyst* **1993,** *118*, 329–334.

(29) Schopf, G., Koâmehl, G. *Polythiophenes—Electrically Conductive Polymers*; Springer: Berlin, 1995.
(30) Nalwa, H. S. *Handbook of Organic Conductive Molecules and Polymers*; John Wiley and Sons: New York, 1997.
(31) Welzel, H. P.; Kossmehl, G.; Schneider, J.; Plieth, W. *Macromolecules* 1995, *28*, 5575–5580.
(32) Hagen, G.; Thoresen, A. H.; Sunde, S.; Hesjevik, S. M.; Odegard, R. *Mol. Cryst. Liq. Cryst.* **1990,** *189*, 213–219.
(33) Zhang, W.; Dong, S. *J. Electroanal. Chem.* **1990,** *284*, 517–521.
(34) Atta, N. F.; Galal, A.; Karagozler, A. E.; Russell, G. C.; Zimmer, H.; Mark, H. B. *Biosens. Bioelectron.* **1991,** *6*, 333–341.
(35) Pietrzyk, A.; Kutner, W.; Chitta, R.; Zandler, M. E.; D'Souza, F.; Sannicolo, F.; Mussini, P. R. *Anal. Chem.* **2009,** *81*, 10061–10070.
(36) Sheats, J. R.; Antoniadis, H.; Hueschen, M.; Leonard, W.; Miller, J.; Moon, R.; Roitman, D.; Stocking, A. *Science* **1996,** *273*, 884–888.
(37) Horowitz, G. *Adv. Mater.* **1998,** *10*, 365–377.
(38) Burroughes, J. H.; Bradley, D. D. C.; Brown, A. R.; Marks, R. N.; Mackay, K.; Friend, R. H.; Burns, P. L.; Holmes, A. B. *Nature* **1990,** *347*, 539–541.
(39) Blanco-Lopez, M. C.; Lobo-Castanon, M. J.; Miranda-Ordieres, A. J.; Tunon-Blanco, P. *Trends Anal. Chem.* **2004,** *23*, 36–48.
(40) Piletsky, S. A.; Turner, A. P. F. *Electroanalysis* **2002,** *14*, 317–323.
(41) Henry, O. Y. F.; Cullen, D. C.; Piletsky, S. A. *Anal. Bioanal. Chem.* **2005,** *382*, 947–956.
(42) Sellergren, B. *Molecularly Imprinted Polymers: Man-made Mimics of Antibodies and their Applications in Analytical Chemistry*; Elsevier: New York, 2000.
(43) Marx, S.; Zaltsman, A.; Turyan, I.; Mandler, D. *Anal.Chem.* **2004,** *76*, 120–126.
(44) Kriz, D.; Ramstrom, O.; Mosbach, K. *Anal. Chem.* **1997,** *69*, 345A–349A.
(45) Baba, A.; Knoll, W.; Advincula, R. *Rev. Sci. Instrum.* **2006,** *77*, 064101-1–064101-6.
(46) Baba, A.; Knoll, W.; Advincula, R. *J. Phys. Chem. B* **2002,** *106*, 1581–1587.
(47) Xia, C.; Advincula, R. C. *Langmuir* **2002,** *18*, 3555–3560.
(48) Park, M.-K.; Youk, J.-H.; Pispas, S.; Hadjichristidis, N.; Advincula, R. C. *Langmuir* **2002,** *18*, 8040–8044.
(49) Bi, X.; Yang, K. *Anal. Chem.* **2009,** *81*, 527–532.
(50) Jenik, M.; Schirhagl, R.; Schirk, C.; Hayden, O.; Lieberzeit, P.; Blaas, D.; Paul, G.; Dickert, F. L. *Anal. Chem.* **2009,** *81*, 5320–5326.
(51) Alexander, C.; Andersson, H. S.; Andersson, L. I.; Ansell, R. J.; Kirsch, N.; Nicholls, I. A.; O'Mahony, J.; Whitcombe, M. J. *J. Mol. Recognit.* **2006,** *19*, 106–180.
(52) Jiang, G.; Baba, A.; Advincula, R. *Langmuir* **2007,** *23*, 817–825.
(53) Taranekar, P.; Baba, A.; Fulghum, T. M.; Advincula, R. C. *Macromolecules* **2005,** *38*, 3679–3687.
(54) Millan, M. D.; Locklin, J.; Fulghum, T.; Baba, A.; Advincula, R. C. *Polymer* **2005,** *46*, 5556–5568.
(55) Wang, E.; Li, G.; Li, D.; Zhai, J.; Zhang, L. *Chem.—Eur. J.* **2009,** *15*, 9868–9873.
(56) Reddy, J. A.; Dean, D.; Kennedy, M. D.; Low, P. S. *J. Pharm. Sci.* **1999,** *88*, 1112–1118.
(57) Ladino, C. A.; Chari, R. V. J.; Bourret, L. A.; Kedersha, N. L.; Goldmacher, V. S. *Int. J. Cancer* **1997,** *73*, 859–864.
(58) Tucker, K. L.; Mahnken, B.; Wilson, P. W. F.; Jacques, P.; Selhub, J. *J. Am. Med. Assoc.* **1996,** *276*, 1879–1885.
(59) Rader, J. I. Issues relating to folic acid fortification of cereal grains products: Update from FDA, Cereal Foods World, 1998; p 545.
(60) Pawlosky, R. J.; Flanagan, V. P. *J. Agric. Food Chem.* **2001,** *49*, 1282–1286.
(61) Sato, K.; Muramatsu, K.; Amano, S. *Anal. Biochem.* **2002,** *308*, 1–4.
(62) Fitzpatrick, J.; Tompsett, S. L. *J. Clin. Pathol.* **1949,** *2*, 121–125.
(63) Harris, D. A. *Anal. Chem.* **1955,** *27*, 1690–1694.
(64) Wright, A. J. A.; Philips, D. R. *Br. J. Nutr.* **1985,** *53*, 569–573.
(65) *State Pharmacopoeia of USSR*, 10th ed.; Ministry of Health: Moscow, Russia, 1968; p 49.
(66) Allfrey, V.; Teply, L. J.; Greffen, C.; King, C. G. *J. Biol. Chem.* **1949,** *178*, 465–481.
(67) Kanjilal, G.; Mahajan, S. N.; Ramana Rao, G. *Analyst* **1975,** *100*, 19–24.
(68) Taranekar, P.; Fulghum, T.; Baba, A.; Patton, D.; Advincula, R. *Langmuir* **2007,** *23*, 908–917.
(69) Taranekar, P.; Fulghum, T.; Baba, A.; Patton, D.; Ponnapati, R.; Clyde, G.; Advincula, R. *J. Am. Chem. Soc.* **2007,** *129*, 12537–12548.
(70) Ulman, A. *An Introduction to Ultrathin Organic Films: From Langmuir—Blodgett to Self Assembly*; Academic: New York, 1991.
(71) Sullivan, J. T.; Harrison, K. E.; Mizzell, J. P., III; Kilbey, S. M., II. *Langmuir* **2000,** *16*, 9797–9803.
(72) Taranekar, P.; Park, J. Y.; Patton, D.; Fulghum, T.; Ramon, J. G.; Advincula, R. C. *Adv. Mater.* **2006,** *18*, 2461–2465.
(73) McCullough, R. D.; Ewbank, P. C.; Loewe, R. S. *J. Am. Chem. Soc.* **1997,** *119*, 633–634.
(74) Bockris, J. O. M.; Khan, S. U. M. *Surface Electrochemistry, A Molecular Level Approach*; Kluwer Academic/Plenum Publishers: New York, 1993.
(75) Buttry, D. A.; Ward, M. D. *Chem. Rev.* **1992,** *92*, 1355–1379.
(76) Geelhood, S. J.; Frank, C. W.; Kanazawa, K. *J. Electrochem. Soc.* **2002,** *149*, 33–38.
(77) Muramatsu, H.; Tamiya, E.; Karube, I. *Anal. Chem.* **1988,** *60*, 2142–2146.
(78) Sauerbrey, G. *Z. Phys.* **1959,** *155*, 206–222.
(79) Xie, C.; Li, H.; Li, S.; Wu, J.; Zhang, Z. *Anal. Chem.* **2010,** *82*, 241–249.
(80) Li, Y.; Yang, H.; You, Q.; Zhuang, Z.; Wang, X. *Anal. Chem.* **2006,** *78*, 317–320.
(81) Sajonz, P.; Kele, M.; Zhong, G.; Sellergren, B.; Guiochon, G. *J. Chromatogr. A* **1998,** *810*, 1–17.
(82) Nicholls, I. A.; Adbo, K.; Andersson, H. S.; Andersson, P. O.; Ankarloo, J.; Hedin-Dahlstrom, J.; Jokela, P.; Karlsson, J. G.; Olofsson, L.; Rosengren, J. *Anal. Chim. Acta* **2001,** *435*, 9–18.
(83) Ferraris, J. P.; Haillon, T. R. *Polymer* **1989,** *30*, 1319–1327.
(84) Yassar, A.; Roncali, J.; Garnier, F. *Macromolecules* **1989,** *22*, 804–809.
(85) Wei, Y.; Chan, C. C.; Tian, J.; Jang, G. W.; Hseuh, K. F. *Chem. Mater.* **1991,** *3*, 888–897.
(86) Riskin, M.; Tel-Vered, R.; Bourenko, T.; Granot, E.; Willner, I. *J. Am. Chem. Soc.* **2008,** *130*, 9726–9733.
(87) Kan, X.; Zhao, Y.; Geng, Z.; Wang, Z.; Zhu, J. *J. Phys. Chem. C* **2008,** *112*, 4849–4854.
(88) Sellergren, B. *Macromolecules* **2006,** *39*, 6306–6309.
(89) McCullough, R. D. *Adv. Mater.* **1998,** *10*, 93–116.
(90) Holdsworth, C. I.; Bowyer, M. C.; Lennard, C.; McCluskey, A. *Aust. J. Chem.* **2005,** *58*, 315–320.
(91) Schwarz, L.; Bowyer, M. C.; Holdsworth, C. I.; McCluskey, A. *Aust. J. Chem.* **2006,** *59*, 129–134.
(92) Schwarz, L.; Holdsworth, C. I.; McCluskey, A.; Bowyer, M. C. *Aust. J. Chem.* **2004,** *57*, 759–764.
(93) Whitcombe, M. J.; Martin, L.; Vulfson, E. N. *Chromatographia* **1998,** *47*, 457–464.
(94) Tanabe, K.; Takeuchi, T.; Matsui, J.; Ikebukuro, K.; Yano, K.; Karube, I. *J. Chem. Soc., Chem. Commun.* **1995,** 2303–2304.
(95) Sellergren, B.; Lepisto, M.; Mosbach, K. *J. Am. Chem. Soc.* **1988,** *110*, 5853–5960.
(96) Lepisto, M.; Sellergren, B. *J. Org. Chem.* **1989,** 6010–6012.
(97) Sarneski, J. E.; Surprenant, H. L.; Reilley, C. N. *Spectrosc. Lett.* **1976,** *9*, 885–894.
(98) Yonezawa, T.; Morishima, I.; Takeuchi, K. *Bull. Chem. Soc. Jpn.* **1967,** *40*, 1807–1813.
(99) Rebek, J., Jr.; Askew, B.; Killoran, M.; Nemeth, D.; Lin, F. T. *J. Am. Chem. Soc.* **1987,** *109*, 2426–2431.
(100) Manesiotis, P.; Hall, A. J.; Sellergren, B. *J. Org. Chem.* **2005,** *70*, 2729–2738.

(101) Berlin, A. In *Electrical and Optical Polymer Systems—Fundamentals, Methods and Applications*; Wise, D. L., Wner, G. E., Trantolo, D. J., Cooper, T. M., Gresser, J. D., Eds.; Marcel Dekker: New York, 1993; p 47.
(102) Willicut, R. J.; McCarley, R. L. *Adv. Mater.* **1995,** *7*, 759–762.
(103) Lukkari, J.; Alanko, M.; Pitkanen, V.; Kleemola, K.; Kankare, J. *J. Phys. Chem.* **1994,** *98*, 8525–8535.
(104) Xia, C.; Fan, X.; Park, M.; Advincula, R. C. *Langmuir* **2001,** *17*, 7893–7898.
(105) Schwartz, B. J. *Annu. Rev. Phys. Chem.* **2003,** *54*, 141–172.
(106) Beamson, G.; Briggs, D. *High Resolution XPS of Organic Polymers: The Scienta ESCA 300 Database*; John Wiley & Sons Ltd.: Chichester, U.K., 1992.
(107) Wojtowicz, M. A.; Pels, J. R.; Moulijn, J. A. *Fuel* **1995,** *74*, 507–516.
(108) Cutivet, A.; Schembri, C.; Kovensky, J.; Haupt, K. *J. Am. Chem. Soc.* **2009,** *131*, 14699–14702.
(109) Qin, L.; He, X.-W.; Zhang, W.; Li, W.-Y.; Zhang, Y.-K. *Anal. Chem.* **2009,** *81*, 7206–7216.
(110) Bolisay, L. D.; Culver, J. N.; Kofina, P. *Biomacromolecules* **2007,** *8*, 3893–3899.
(111) Ceolin, G.; Navarro-Villoslada, F.; et al. *J. Comb. Chem.* **2009,** *11*, 645–652.
(112) Kobayashi, T.; Reddy, P. S.; Ohta, M.; Abe, M.; Fujii, N. *Chem. Mater.* **2002,** *14*, 2499–2505.
(113) Kaiser, H. *Anal. Chem.* **1970,** *42*, 26A–59A.
(114) Long, G. L.; Winefordner, J. D. *Anal. Chem.* **1983,** *55*, 712A–724A.
(115) Thomsen, V.; Schatzlein, D.; Mercuro, D. *Spectroscopy* **2003,** *18*, 112–114.
(116) Skoog, D. A.; Holler, F. J.; Nieman, T. A. *Principles of Instrumental Analysis*; Harcourt Asia PTE Ltd.: Mumbai, India, 1998; p 13.
(117) Batra, D.; Shea, K. J. *Current Opin. Chem. Biol.* **2003,** *7*, 434–442.
(118) Vlatakis, G.; Andersson, L. I.; Muller, R.; Mosbach, K. *Nature* **1993,** *361*, 645–647.
(119) Wyman, J. *Adv. Protein Chem.* **1964,** *19*, 223.
(120) Heck, H. d'A. *J. Am. Chem. Soc.* **1971,** *93*, 23–29.
(121) Kamikawa, Y.; Nishii, M.; Kato, T. *Chem.—Eur. J.* **2004,** *10*, 5942–5951.